sciendo

LATVIAN JOURNAL OF PHYSICS
AND TECHNICAL SCIENCES
2025, N 1

DOI: 10.2478/lpts-2025-0001

OPTIMISATION AND SYNTHESIS OF SINGLE BLADE VIBRATION MOTION IN AIRFLOW

V. Beresnevics[1*], J. Viba[1], M. Irbe[1], M. Cerpinska[1], S.K. Vutukuru[2]

[1]Riga Technical University,
Institute of Mechanical and Biomedical Engineering,
6B Kipsalas Str., Riga, LV-1048, LATVIA
[2]MVJ College of Engineering,
Department of Aerospace,
Bengaluru, 560012, INDIA
*e-mail: vitalijs.beresnevics@rtu.lv

The study focuses on wind flow energy harvesting technology utilising the vibration method. The one-degree-of-freedom mathematical model comprises a flat plate connected to a foundation via an elastic element, subjected to airflow induced by the wind. Energy accumulation occurs within a generator. The braking force exerted by the generator can assume a constant, linear, or non-linear relationship with plate velocity. Oscillation motion is induced by altering the plate area within each oscillation cycle, with maximum area exposure to the windward motion and minimum during leeward movement. Control switches, functioning as level functions, facilitate motion synthesis and simulation by simplifying the description of plate area and generator switching control in the phase plane. Additionally, a control switching delay is introduced for plate area variation, described in terms of velocity and coordinate levels. The paper presents computer simulation results in the form of phase diagrams and time responses, followed by an analysis of generated power and energy extraction efficiency.

Keywords: *Air flow, energy harvesting, plate vibrations, surface area control, switching delay.*

1. INTRODUCTION

In recent times, there has been a notable surge in interest regarding the deployment and integration of small or medium-sized wind energy harvesting equipment within urban settlements [1]. This study evaluates the performance of wind turbines and technologies that utilise micro or small wind-induced vibrations to improve their efficiency and reliability in operation. Wind energy harvesting technologies based on the use of interaction forces between air flow and moving objects through reciprocating motions demonstrate a wide range of approaches. For instance, research [2]–[7] delves into the examination of vibrations characterised by flapping or fluttering. Accordingly, investigations into the utilisation of vortices-induced vibrations can be found in studies [8]–[12], while galloping mechanisms are explored, for example, in works [13]–[17]. The analysis of these studies reveals that rotating turbines, whether vertically or horizontally oriented, generally exhibit higher power outputs compared to vibration-based technology equipment, owing to the absence of blade-stopping moments. Nevertheless, rotating turbines also present certain drawbacks [18] listed below.

- They can attain high speeds at the radial extremities, potentially posing hazards to nearby living or inanimate objects.
- High speeds may lead to increased blade vibrations and noise levels.
- Their proximity to residential structures is not always desirable.

However, vibration-based wind energy harvesting equipment also carries its own set of limitations [19] presented below.

- The energy gained during the downwind phase is reduced by the energy expanded during the upwind phase.
- Energy production levels are generally lower compared to rotor-type turbines.
- Possibility of additional high-frequency noise and vibrations.
- Sensitivity of vibration amplitudes to changes in wind speed.

To improve the efficiency of oscillatory motion technology in extracting wind energy, this study uses the principles of optimal synthesis [20], [21]. For this purpose, changing the surface area of the oscillating plate is chosen as a control action [22]. In addition, the energy storage generator control is designed with adjustable operating thresholds. Since in a real mechanism it is physically impossible to change the surface area instantly (bang-bang control), computer simulations include a delay in switching areas to simulate motion [23].

2. MOTION CONTROL OPTIMISATION

A model depicting the movement of a plate along the Ox direction is shown in Fig. 1. This model comprises a plate 2, which moves along the x-axis and is connected to an actuator 3. A wind flow with velocity V_0 acts on the plate at the angle β relative to x axis. The actuator 3 serves to simulate the force produced by the energy generator, as well as additional damping forces within the system. The forward motion of the system, when the relative wind velocity projections to the normal and plate are positive, is described by the following differential equation [24], [25]:

$$m\ddot{x} = A\rho(1+C)(V_0\cos\beta - \dot{x})^2 - F_G - F_D, \quad (1)$$

where m being the mass of moving plate, kg; x is a displacement of the plate, m; C is a dimensionless constant; A is the plate lateral surface area, m^2; ρ is the air density, kg/m^3; V_0 is the air flow velocity, m/s; β is the angle between airflow velocity and x axis, rad; F_G is the force of energy generator and F_D *is* the additional damping force, N.

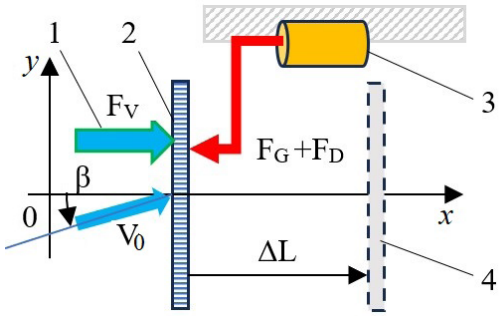


Fig. 1. A schematic diagram of plate rectilinear movement system: 1 – wind interaction force; 2 – a thin flat plate; 3 – an energy storage and damping actuator; 4 – end position of the plate.

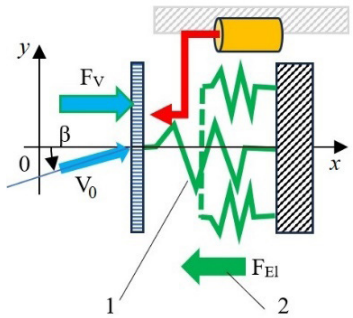


Fig. 2. Reciprocating vibrating system: 1 – a non-linear spring system; 2 – spring force.

The equation of motion of the reciprocating vibrating system (Fig. 2) is similar to Eq. (1), but it is supplemented with the force F_{EL} of the flexible element and with the sign function (±1) switching the direction of relative velocity ($V_0\cos\beta - \dot{x}$):

$$m\ddot{x} = A\rho(1+C)(V_0\cos\beta - \dot{x})^2 \cdot \mathrm{sign}(V_0\cos\beta - \dot{x}) - F_G - F_D - F_{EL}\,. \quad (2)$$

Examining Eq. (1) through the lens of control optimisation [20], [21], it is possible to select the area $A = u_1 \cdot m[\rho(1+C)]^{-1}$ and the force $F_G = mu_2$ as control functions dependent on time t and phase coordinates $x, \dot{x}$, denoted as $u_1 = u_1(t, x, \dot{x})$, $u_2 = u_2(t, x, \dot{x})$, respectively. In the scenario of unidirectional stationary motion, the criterion should reflect the energy obtained from the generator, expressed in the following form [22]:

$$J(x, \dot{x}, u_1, u_2) = \int_{t1}^{t2} u_2 \dot{x} dt, \quad (3)$$

where t_1 and t_2 are the start and end times of the movement under consideration, when the displacement ΔL is performed (Fig. 1).

The stated optimisation problem imposes a constraint on the size of the positive area A with minimal $u_1^{(1)}$ and maximal $u_1^{(2)}$ values, in accordance with the following equation:

$$[u_1^{(1)}] \le u_1 \le [u_1^{(2)}]. \quad (4)$$

In terms of generator control, it is established that $u_2 > 0$. However, the maximum value is limited by the operational capacity of the mechanism to manoeuvre within the

airflow, as outlined in the following equation:

$$0 \le u_2 \le [u_2^{(0)}]. \quad (5)$$

During the optimisation process of system control variables u_1 and u_2, the Pontryagin's maximum principle is applied, particularly in strongly nonlinear scenarios [22]. For this purpose, Eq. (1) is reformulated in terms of derivatives with respect to phase coordinates, including an additional function under the integral, as described in Eq. (3). As a result, the following system of equations is obtained:

$$\begin{aligned} \frac{dx_0}{dt} &= u_2 x_2; \\ \frac{dx_1}{dt} &= x_2; \\ \frac{dx_2}{dt} &= u_1 \cdot (V_0 \cos\beta - x_2)^2 \cdot (+1) - u_2 - F_D m^{-1}, \end{aligned} \quad (6)$$

where (+1) means that the relative velocity is positive.

According to the optimization theory [22], the Hamiltonian H, studied here is as follows:

$$H = \psi_0 u_2 x_2 + \psi_1 x_2 + \psi_2 \{u_1 (V_0 \cos\beta - x_2)^2 \cdot (+1) - u_2 - F_D m^{-1}\}. \quad (7)$$

Here the components ψ_0, ψ_1, ψ_2 of the related function ψ are found from their derivatives by the time t as follows [21], [22]:

$$\frac{d\psi_0}{dt} = -\frac{\partial H}{\partial x_0}; \ \frac{d\psi_1}{dt} = -\frac{\partial H}{\partial x_1}; \ \frac{d\psi_2}{dt} = -\frac{\partial H}{\partial x_2}, \quad (8)$$

where $\frac{\partial H}{\partial x_0}, \frac{\partial H}{\partial x_1}, \frac{\partial H}{\partial x_2}$ are the partial derivatives of H by coordinates x_0, x_1 , x_2.

According to the optimisation theory, for optimal control at any given time moment t, function H must reach its maximum (or supremum) value subject to the constraints specified in Eqs. (4) and (5).

Analysing such a task in stationary motion with constant blade speed V_{opt} = const, when $F_D = 0$, the following optimal solution can be found:

$$V_{opt} = \frac{V_0 \cos\beta}{3}; \quad (9)$$

$$F_{Dopt} = A_{max} \cdot \rho(1 + C) \left[\frac{2}{3} V_0 \cos\beta\right]^2; \quad (10)$$

$$P_{opt} = A_{max} \cdot \rho(1 + C) \frac{4}{27} \cdot [V_0 \cos\beta]^3, \quad (11)$$

where A_{max} is the plate maximal area, F_{Dopt} is the required force from the power generator, and P_{opt} is the maximum generated power in the optimisation case.

Thus, if the damping force F_D is neglected, the operating force F_G of the generator can be selected. Since in practice there are uncontrollable damping forces F_D, the generator force F_G will correspondingly decrease by this amount. It should be noted that during the transition process, additional

optimisation of the system is possible, for example, starting movement from a stationary position and moving to the supposed optimal position. In such scenarios, the optimisation criterion may not prioritise energy as shown in Eq. (3), but rather focus on minimising travel time T. Therefore, in the optimisation process, the expression in Eq. (3) should be replaced by the following expression:

$$J(x, \dot{x}, u_1, u_2) = \int_0^T 1 \cdot dt. \tag{12}$$

It is clear that in this optimal control scenario, the area A should be maximised (A_{max}), while the energy generator force must be set to zero ($u_2 = 0$). Following the attainment of the previously determined optimal stationary state, the generator should be engaged with the optimal force for mechanism synthesis. Considering the optimisation outcome obtained earlier, it can be inferred that the generator's characteristics offer a wide range of possibilities: it could function as a constant force, a linear or nonlinear function of velocity, or adopt other configurations. The application of the optimisation results discussed previously to the synthesis of wind energy harvesting mechanisms is detailed in studies [25]–[27].

Accordingly, the synthesis of the mechanism involving reciprocating vibrational motion (Fig. 2) is discussed in detail below.

3. MOTION MODELLING AND PARAMETER OPTIMISATION FOR OSCILLATORY SYSTEM SYNTHESIS

During the modelling and parameter optimisation, the following differential equation of motion for $\beta = 0$ was initially analysed:

$$m\ddot{x} = A\rho(1 + C)\{b_0 + b_1[0.5 \cdot \text{sign}(\dot{x} - \Delta) + 0.5 \cdot \text{sign}(\dot{x} + \Delta)]\} \cdot (V_0 - \dot{x})^2 \cdot \\ \cdot \text{sign}(V_0 - \dot{x}) - b_2\dot{x} - cx, \tag{13}$$

where b_0, b_1, Δ are the constants of the control switching function of area A, b_2 is the linear generator parameter, c is the linear elasticity parameter or linear spring stiffness coefficient.

The simulation was performed with computer program MathCad under the following constant parameters: m = 100 kg; A = 1 m^2; ρ = 1.25 kg/m^3; C = 0.25; b_0 = 1. The remaining parameters (V_0, b_1, Δ, b_2, c) were varied. The results of modelling of free oscillations (for $b_1 = 0$) are presented in Figs. 3–5.

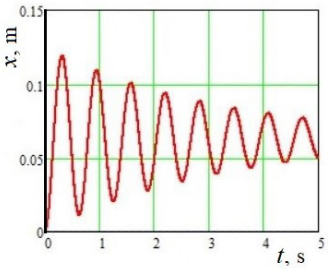


Fig. 3. The displacement x of the plate as a function of time t under the conditions V_0 = 20 m/s, $b_1 = 0$, $b_2 = 0$.

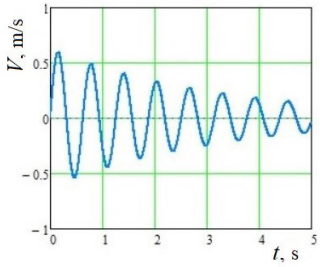


Fig. 4. Velocity of the plate V as a function of time t under the conditions V_0 = 20 m/s, $b_1 = 0$, $b_2 = 0$.

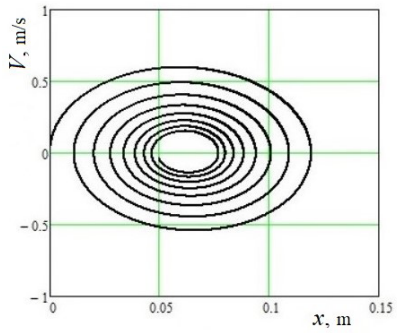


Fig. 5. Reciprocating motion in phase plane (x, V): $V_0 = 20$ m/s, $b_1 = b_2 = 0$.

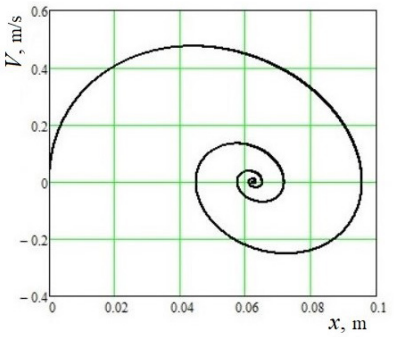


Fig. 6. Motion in phase plane (x, V): $V_0 = 20$ m/s, $b_1 = 0$ and $b_2 = 333.3$ kg/s.

From the graphs depicted in Figs. 3–5, it is evident that the interaction of the plate with airflow, even when the generator is inactive ($b_2 = 0$), exerts a considerable damping effect. Consequently, other drag forces can be disregarded ($F_D = 0$) for further analysis. However, in a practical scenario, the energy required for transitioning between areas should be assessed as a partial deduction from the overall energy yield (Fig. 6). Subsequent to this assessment, Figs. 7 and 8 present modelling outcomes derived from optimising the energy harvesting generator. These results pertain to a linear generator configuration under the conditions: $V_0 = 20$ m/s, $b_0 = 1$, $b_1 = 0.8$, $b_2 = 350$ kg/s, $\Delta = 0.1$.

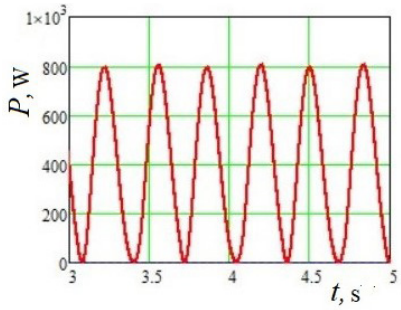


Fig. 7. Variation of power P in time t.

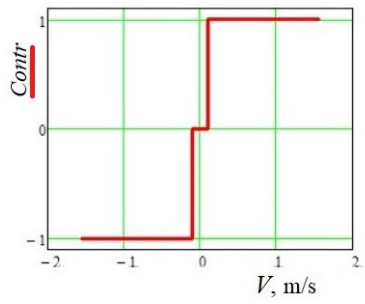


Fig. 8. The plate shutter switching control as a function of velocity V.

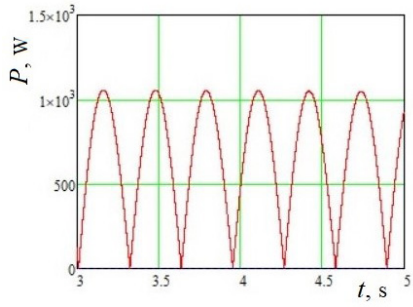


Fig. 9. Variation of power P in time t.

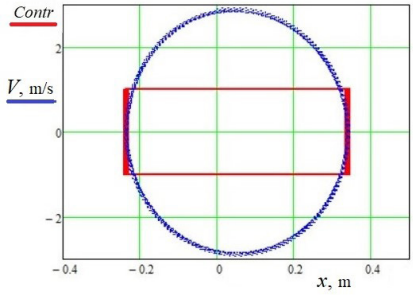


Fig. 10. The plate switching control in velocity $V=\dot{x}$ domain.

As follows from Fig. 7, the average power is P_m = 413 W. Furthermore, the power efficiency of the process, concerning optimal rectilinear motion in accordance with Eq. (11), stands at E_f = 22.32 %. However, plate shutter switching control (Fig. 8) is performed as a function of velocity in accordance with Eq. (13): $Contr = b_0 + b_1[0.5 \cdot \text{sign}(\dot{x} - \Delta) + 0.5 \cdot \text{sign}(\dot{x} + \Delta)]$.

In Figs. 9 and 10, modelling results are presented, derived from the optimisation of an energy harvesting generator configured with a nonlinear characteristic, such as dry friction $F_G = B \cdot \text{sign}(\dot{x})$. These results are obtained under the conditions: V_0 = 20 m/s, b_0 = 1, b_1 = 0.8, b_2 = 350 kg/s, Δ = 0.1, and B = 370 N. The power P graph (Fig. 9) indicates an average power output of 705 W. Furthermore, the power efficiency of the process, relative to the optimal rectilinear motion with Eq. (11), is calculated as E_f = 38 %. However, plate switching control in velocity domain (Fig. 10) is performed with Eq. (13): $Contr = b_0 + b_1[0.5\text{sign}(\dot{x} - \Delta) + 0.5\text{sign}(\dot{x} + \Delta)]$.

Upon comparing the results obtained with both a linear and a non-linear generator, it becomes evident that in the latter case, there is a potential to elevate the average energy efficiency E_f from 22 % to 38 %. The subsequent section addresses how further enhancements in energy production efficiency can be achieved by altering the operational control of the generator.

4. RESULTS AND DISCUSSION

It is worth mentioning that in oscillating motion with mechatronic control, it is feasible to electrically toggle the generator on or off using a "bang–bang" control approach [28]. For example, it is viable to activate periodically the generator at specific movement velocity thresholds, as described by the following equation:

$$F_G = B \cdot \text{sign}(\dot{x}) \cdot [0.5 + 0.5 \cdot \text{sign}(|\dot{x}| - \Delta_1)], \quad (14)$$

where Δ_1 is a constant velocity level, m/s.

Thus, through optimisation of the parameter Δ_1, an optimal value of Δ_1 = 5.25 m/s was achieved, yielding a power output of 1032 W and an efficiency of E_f = 55.7 %. Accompanying this optimisation, the graph depicting the control function, as per Eq. (14), is illustrated in Fig. 11. The power graph for the optimal movement scenario is presented in Fig. 12.

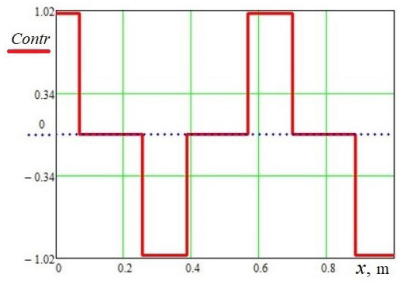


Fig. 11. Graph of the "bang–bang" control function as defined by Eq. (14).

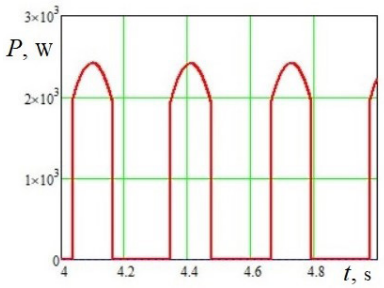


Fig. 12. Power graph for the optimal movement scenario: V_0 = 20 m/s, b_0 = 1, b_1 = 0.8, b_2 = 350 kg/s, Δ = 0.1, B = 370 N, Δ_1 = 5.25 m/s, E_f = 55.7 %.

Continuing with the synthesis process of the energy harvesting system F_G, an analysis of the elastic force F_{EL} for the cubic form was conducted, as described by the following equation:

$$F_G + F_{EL} = B\text{sign}(\dot{x}) \cdot [0.5 + 0.5 \cdot \text{sign}(|\dot{x}| - \Delta_1)] + c_1 x^3, \quad (15)$$

where c_1 is the nonlinear elasticity parameter, kg/s^2.

In this context, an illustrative example depicting movement in the phase plane from a stationary state is presented in Fig. 13. Subsequently, the power graph obtained through the "bang–bang" connection of the electric generator is shown in Fig. 14. In accordance with simulation results, a medium power output is about 1063 W and efficiency is of E_f = 57.4 %.

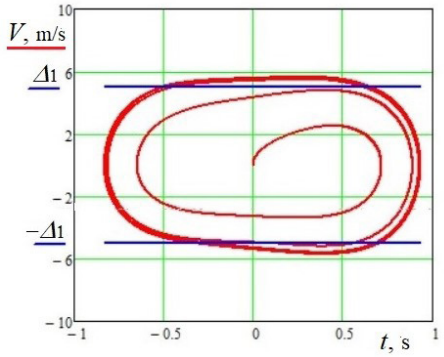


Fig. 13. Motion in the phase plane for the optimal movement scenario (c_1 = 10000 kg/s^2; Δ_1 = 5 m/s), when: V_0 = 20 m/s, b_0 = 1, b_1 = 0.8, b_2 = 350 kg/s, Δ = 0.1, B = 370 N.

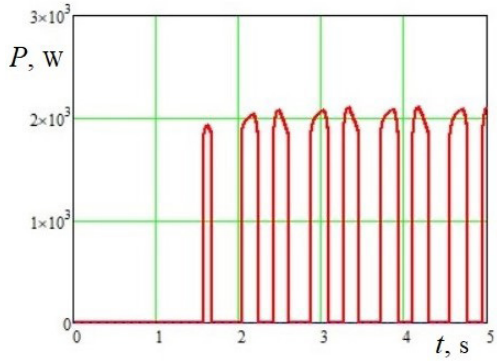


Fig. 14. Power graph for the optimal movement scenario with c_1 = 10000 kg/s^2 and Δ_1 = 5 m/s.

In the numerical analysis, it was determined that the elastic force parameter c_1, within a considerable range of variations ($5 \cdot 10^3$ kg/s^2 < c_1 < $20 \cdot 10^3$ kg/s^2), did not exert a substantial influence on energy recovery (52 % < E_f < 57 %). This is primarily attributed to the conservative nature of the suspension force. However, the investigation did not delve into the implications of a flexible nonlinear suspension in alternative scenarios.

5. CONCLUSIONS

As the scope of energy extraction from airflow expands, there is growing interest in optimising the operation of existing equipment and synthesising new machinery. Mechatronic control systems offer a promising avenue for achieving these goals. In the operating principles of existing systems, it is crucial to study variation in the area of interaction between the airflow and the object. Moreover, there is a need to explore control synthesis in mechatronic systems. As such, it is suggested to implement varia-

tions in the interaction area between the airflow and objects while considering control delays. Additionally, the application of bang–bang control for energy generators is under consideration. The research findings are outlined as follows:

1. optimisation of the control for varying the interaction area and managing the energy generator has been carried out.
2. during the synthesis of new equipment, it is suggested to incorporate observation of a control delay using a three-level function (+1; 0; -1) while adjusting the interaction area;
3. when synthesizing real equipment, bang–bang control is used, which increases the efficiency of the energy production system.

REFERENCES

1. Calautit, K., & Johnstone, C. (2023). State-of-the-art Review of Micro to Small-scale Wind Energy Harvesting Technologies for Building Integration. *Energy Conversion and Management: X*, *20* (100457), 1–29. https://doi.org/10.1016/j.ecmx.2023.100457
2. Chawdhury, S., & Morgenthal, G. (2018). Numerical Simulations of Aeroelastic Instabilities to Optimize the Performance of Flutter-based Electromagnetic Energy Harvesters. *Journal of Intelligent Material Systems and Structures*, *29* (4), 479–495. https://doi.org/10.1177/1045389X17711784
3. Aquino, A., Calautit, J., & Hughes, B. (2017). A Study on the Wind-induced Flutter Energy Harvester (WIFEH) Integration into Buildings. *Energy Procedia*, *142*, 321–327. https://doi.org/10.1016/j.egypro.2017.12.051
4. Aquino, A.I., Calautit, J.K., & Hughes, B.R. (2017). Evaluation of the Integration of the Wind-induced Flutter Energy Harvester (WIFEH) into the Built Environment: Experimental and Numerical Analysis. *Applied Energy*, *207*, 61–77. https://doi.org/10.1016/j.apenergy.2017.06.041
5. Bai, Y., & Zheng, M. (2022). Energy Harvesting Characteristics of a Flapping Wing with the Oscillating Aspirators in Uniform Flows and Shear Flows. *Energy Reports*, *8*, 9554–9568. https://doi.org/10.1016/j.egyr.2022.07.061
6. Zheng, M., Bai, Y., Zhao, T., & Wang, M. (2022). Energy Harvesting Properties of a Flapping Foil with Blow Aspirators: A Numerical Investigation. *Energy Reports*, *8*, 1803–1815. https://doi.org/10.1016/j.egyr.2022.01.003
7. Li, S., Yuan, J., & Lipson, H. (2011). Ambient Wind Energy Harvesting Using Cross-Flow Fluttering. *Journal of Applied Physics*, *109* (2), 026104. https://doi.org/10.1063/1.3525045
8. Naseer, R., Dai, H.L., Abdelkefi, A., & Wang, L. (2017). Piezomagnetoelastic Energy Harvesting from Vortex-Induced Vibrations Using Monostable Characteristics. *Applied Energy*, *203*, 142–153. https://doi.org/10.1016/j.apenergy.2017.06.018
9. Hernandez, R., Jung, S., & Matveev, K.I. (2011). Acoustic Energy Harvesting from Vortex-Induced Tonal Sound in a Baffled Pipe. *Proceedings of the Institution of Mechanical Engineers*, *Part C: Journal of Mechanical Engineering Science*, *225* (8), 1847–1850. https://doi.org/10.1177/0954406211406017
10. Haobo, H., Di, C., Zhiyong, Z., & Wenfeng, D. (2023). Research Progress of Piezoelectric Wind Energy Harvesters Based on Vortex-Induced Vibration. *Chinese Journal of Theoretical and Applied Mechanics*, *55* (10), 2132–2145. https://doi.org/10.6052/0459-1879-23-364
11. Jin, Z., Li, G., Wang, J., & Zhang, Z. (2019). Design, Modeling, and Experiments of the Vortex-Induced Vibration Piezoelectric Energy Harvester with Bionic Attachments. *Complexity,* ID 1670284, 1–13. https://doi.org/10.1155/2019/1670284

12. Hu, Y., Yang, Chen, B.X., Wang, X., & Liu, J. (2018). Modeling and Experimental Study of a Piezoelectric Energy Harvester from Vortex Shedding-Induced Vibration. *Energy Conversion Management, 162*(1), 145–158. https://doi.org/10.1016/j.enconman.2018.02.026
13. Wang, W., Huang, J., & Yao, Z. (2021). Cut-Corner Prism Piezoelectric Energy Harvester Based on Galloping Enhancement Mechanism. *Energy Reports*, *7*, 6366–6374. https://doaj.org/article/87a1ad13e4ba4f419384aeb9af8e9301
14. Barrero-Gil, A., Alonso, A.G., & Sanz-Andres, A. (2010). Energy Harvesting from Transverse Galloping. *Journal of Sound and Vibration*, *329* (14), 2873–2883. https://doi.org/10.1016/j.jsv.2010.01.028
15. Abdelmoula, H., & Abdelkefi, A. (2016). The Potential of Electrical Impedance on the Performance of Galloping Systems for Energy Harvesting and Control Applications. *Journal of Sound and Vibration*, *370*, 191–208. https://doi.org/10.1016/j.jsv.2016.01.037
16. Abdelkefi, A., Hajj, M.R., & Nayfeh, A.H. (2012). Power Harvesting from Transverse Galloping of Square Cylinder. *Nonlinear Dynamics*, *70*, 1355–1363. https://doi.org/10.1007/s11071-012-0538-4
17. Le, H.D., & Kwon, S.-D. (2021). Design and Experiments of a Galloping-Based Wind Energy Harvester Using Quadruple Halbach Arrays. *Energies*, *14* (19), 1–14. https://doi.org/10.3390/en14196094
18. Musial, W., & Ram, B. (2010). *Large-Scale Offshore Wind Power in the United States. Assessment of Opportunities and Barriers*. Report NREL/TP-500-40745. Golden, Colorado 80401, USA: National Renewable Energy Laboratory, 240 p. Available at https://www.nrel.gov/docs/fy10osti/40745.pdf
19. Li, Z., Zhou, S. & Yang, Z. (2022). Recent Progress on Flutter-Based Wind Energy Harvesting. *International Journal of Mechanical System Dynamics*, *2* (1), 82–98. https://doi.org/10.1002/msd2.12035
20. Lavendelis, E., & Viba, J. (2009). Optimal Synthesis Method for Invention of New Mechatronic Systems in Vibrotechnics. *Solid State Phenomena*, *147–149*, 432–437. https://doi.org/10.4028/www.scientific.net/SSP.147-149.432
21. Viba, J. (1988). *Optimization and Syntheses of Vibration Shock Machines*, (in Russian). Latvia, Riga: Zinatne.
22. Boltyanski, V.G., Gamkrelidze, R.V., Mishchenko, E.F., & Pontryagin, L.S. (1960). The maximum principle in the theory of optimal processes of control. *IFAC Proceedings*, *1* (1), 464–469.
23. Park, J.H., Lee, T.H., Liu, Y., & Chen, J. (2019). *Dynamic Systems with Time Delays: Stability and Control*. Berlin: Springer.
24. Viba, J., Beresnevich, V., & Irbe, M. (2020). Synthesis and optimization of wind energy conversion devices. In Maalawi, K.Y. (ed.), *Design Optimization of Wind Energy Conversion Systems with Applications*. London, UK: IntechOpen, 125–141. http://dx.doi.org/10.5772/intechopen.90819
25. Beresnevich, V., Cerpinska, M., Viba, J., & Irbe M. (2022). Dynamics Analysis and Structural Synthesis of Wind Energy Production Device with Closed Loop Conveyor. *Vibroengineering Procedia*, *44*, 156–162. https://www.extrica.com/article/22867
26. Viba, J., Beresnevich, V., Noskovs, S., & Irbe, M. (2016). Investigations of Rotating Blade for Energy Extraction from Fluid Flow. *Vibroengineering Procedia*, *8*, 312–315. https://www.extrica.com/article/17676
27. Viba, J., Beresnevich, V., Irbe, M., & Dobelis, J. (2017). The Control of Blades Orientation to Air Flow in Wind Energetic Device. *Energy Procedia*, *128*, 302–308. https://doi.org/10.1016/j.egypro.2017.08.317
28. Ratmarao, N., & Reitan, D. (1970). Improvement of Power System Transient Stability Using Optimal Control: Bang-Bang Control of Reactance. *IEEE Transactions on Power Apparatus and Systems*, *PAS-89* (5), 975–948.